Journal of Biomechanics ▮ (▮▮▮▮) ▮▮▮–▮▮▮

Contents lists available at ScienceDirect

Journal of Biomechanics

journal homepage: www.elsevier.com/locate/jbiomech
www.JBiomech.com

Comparison of analytical and inverse finite element approaches to estimate cell viscoelastic properties by micropipette aspiration

Ruogang Zhao [a], Kristine Wyss [a,b], Craig A. Simmons [a,b,c,*]

[a] Institute of Biomaterials and Biomedical Engineering, University of Toronto, Toronto, ON, Canada
[b] Department of Mechanical and Industrial Engineering, University of Toronto, Toronto, ON, Canada
[c] Faculty of Dentistry, University of Toronto, Toronto, ON, Canada

ARTICLE INFO

Article history:
Accepted 29 July 2009

Keywords:
Cell mechanics
Micropipette aspiration
Finite element analysis
Viscoelasticity

ABSTRACT

The viscoelastic properties of cells are important in predicting cell deformation under mechanical loading and may reflect cell phenotype or pathological transition. Previous studies have demonstrated that viscoelastic parameters estimated by finite element (FE) analyses of micropipette aspiration (MA) data differ from those estimated by the analytical half-space model. However, it is unclear whether these differences are statistically significant, as previous studies have been based on average cell properties or parametric analyses that do not reflect the inherent experimental and biological variability of real experimental data. To determine whether cell material parameters estimated by the half-space model are significantly different from those predicted by the FE method, we implemented an inverse FE method to estimate the viscoelastic parameters of a population of primary porcine aortic valve interstitial cells tested by MA. We found that inherent differences between the analytical and inverse FE estimation methods resulted in statistically significant differences in individual cell properties. However, in cases with small pipette to cell radius ratios and short loading periods, model-dependent differences were masked by experimental and cell-to-cell variability. Analytical models that account for finite cell-size and loading rate further relaxed the experimental conditions for which accurate cell material parameter estimates could be obtained. These data provide practical guidelines for analysis of MA data that account for the wide range of conditions encountered in typical experiments.

1. Introduction

Characterization of cell viscoelastic properties is required to predict cell deformation under applied loads, and may reflect cell phenotype (Darling et al., 2008) or its transition to a pathological state (Ward et al., 1991; Trickey et al., 2000). Among various single cell probing methods, micropipette aspiration (MA) has been used extensively to measure the viscoelastic properties of several cell types (reviewed in (Hochmuth, 2000)) and cellular organelles (Guilak et al., 2000; Rowat et al., 2006; Vaziri and Mofrad, 2007). To estimate viscoelastic material parameters from MA data, the experimental deformation history is typically fit to a linear viscoelastic half-space analytical model (Sato et al., 1990), in which the cell is an infinitely large half-space undergoing infinitesimal deformation and subjected to instantaneously applied pressure. In reality, however, aspirated cells vary in size, undergo large deformations during aspiration, and experimental loading rates are finite, with the pressure typically ramped over several seconds.

To address limitations of the half-space model, finite element (FE) models of single cell (Baaijens et al., 2005; Zhou et al., 2005) and tissue (Aoki et al., 1997; Boudou et al., 2006) MA have been developed. FE models account for realistic geometric constraints, boundary conditions, and material and geometric nonlinearities, which putatively lead to more accurate predictions of material parameters than those obtained analytically. FE analyses have shown that finite cell-size and nonlinearities caused by large deformation, contact slippage, and material properties all potentially impact cell deformation during MA, resulting in material parameter estimates that differ from those predicted analytically. As a result, models that account for finite sample thickness (Alexopoulos et al., 2003; Boudou et al., 2006) and finite cell radius (Zhou et al., 2005) have been proposed. Analytical simulations show that time-dependent effects due to finite loading rates also impact cell properties estimates (Merryman et al., 2009).

While previous studies have demonstrated that material parameters estimated by FE analyses of MA differ from that estimated analytically, it is not clear whether these differences are statistically significant, as simulations rarely reflect the inherent experimental and biological variability of real experimental data. This is an important distinction: if simple analytical models predict material parameters that are statistically indistinguishable from those predicted computationally for typical experimental

* Corresponding author at: Department of Mechanical & Industrial Engineering, University of Toronto, 5 King's College Road, Toronto, ON, Canada, M5S 3G8. Tel.: +416 946 0548; fax: +416 978 7753.
E-mail address: c.simmons@utoronto.ca (C.A. Simmons).

0021-9290/$ - see front matter © 2009 Elsevier Ltd. All rights reserved.
doi:10.1016/j.jbiomech.2009.07.035

conditions, then analytical approaches, which are trivial to apply and available universally, are adequate for material parameter estimation.

The objective of this study was to determine whether viscoelastic material parameters estimated analytically differ significantly from those predicted by the finite element method for a population of cells tested by MA. In the latter case, material parameters were estimated by nonlinear regression of experimental data using an inverse FE method. Statistical comparisons were made over a range of typical experimental conditions that included variable cell-sizes and finite loading rates. The results provide practical guidelines for the analysis of MA data.

2. Materials and methods

Detailed methods are described in the Supplemental Material.

2.1. Experimental methods

Primary porcine aortic valve interstitial cells (VICs) were isolated by collagenase digestion (Yip et al., 2009) and tested within 3 h of isolation. Micropipette aspiration was conducted using a custom-built system similar to those described previously (Trickey et al., 2000). Twenty-five VICs were tested by applying a single ramp increase of 515.9 ± 7.6 Pa over periods of 2 s (n=7) or 8 s (n=18), followed by equilibration for a minimum of 120 s.

2.2. Standard half-space and other analytical models

A linear viscoelastic half-space model was used to fit the deformation history of a VIC subjected to an instantaneous aspiration pressure (Sato et al., 1990; Guilak et al., 1999). In this model the normalized aspiration length of the cell is given as

$$\frac{L}{R_p} = \frac{\phi_p \Delta P}{2\pi G_0(1-\alpha_1)}[1-\alpha_1 e^{-t/\tau}] \quad (1)$$

where Φ_p is a wall function (assumed to be a constant value of 2.1 (Theret et al., 1988)), L the aspiration length, R_p the pipette radius, ΔP the applied pressure, G_0 the instantaneous shear modulus, α_1 the dimensionless relaxation modulus, and τ the creep time constant. The viscoelastic parameters G_0, α_1 and τ of an individual cell were determined by fitting the experimental deformation history of the cell to Eq. (1) using a nonlinear least-squares method (Matlab, The MathWorks, Inc., Natick, MA).

Cell material property estimates were also obtained using the thickness-corrected half-space model proposed by Boudou et al. (2006) and the cell-size-corrected relationships proposed by Zhou et al. (2005). To account for the finite loading rates, Boltzmann superposition was incorporated into the half-space model to account for creep during loading, as described by Merryman et al. (2009). In this model, the normalized aspiration length of a VIC subjected to a linear ramp pressure ($\Delta P = c\,t$) during the loading period (2 or 8 s in this study) is given as:

$$\frac{L(t)}{R_p} = \frac{\phi_p c}{2\pi G_0(1-\alpha_1)}[t-\alpha_1\tau(1-e^{-t/\tau})] \quad (2)$$

Viscoelastic parameters in Eq. (2) were determined using a nonlinear least-squares curve fitting method in Matlab.

2.3. Finite element model

In the FE model, the cell was assumed to be a deformable sphere having isotropic and homogeneous material properties. The material properties of the cell were described by a finite strain viscoelastic model, which is a time domain generalization of a nearly incompressible (Poisson's ratio v=0.499) hyperelastic neo-Hookean constitutive model (ABAQUS, 2006). The relaxation shear modulus $G(t)$ of the finite strain viscoelastic model was represented by a one-term Prony series as

$$G(t) = G_0[1-\alpha_1(1-e^{-(t/(1-\alpha_1)\tau)})] \quad (3)$$

The FE analysis was performed using ABAQUS (ABAQUS, Inc., Providence, RI).

2.4. Inverse finite element method

The inverse FE analysis involves the coupling of a forward FE analysis that predicts model response based on the input material parameters and an optimization algorithm that finds the "best-fit" material parameters by minimizing the error between the model-predicted response and the experimental measurement (Kyriacou et al., 1997; Lei and Szeri, 2007). This procedure was implemented using the Levenberg–Marquardt algorithm in a Matlab routine that was coupled with ABAQUS.

2.5. Comparison of analytical and numerical model predictions and the effect of loading rate

The viscoelastic parameters predicted by the standard half-space model (Sato et al., 1990), the Boudou finite-thickness-corrected model (Boudou et al., 2006), the Zhou finite cell-size-corrected model (Zhou et al., 2005), and the inverse FE method for individual VICs (tested with 2 s loading period) were compared, based on the assumption in the models of instantaneous loading. Comparisons were made on the goodness of fit and the optimized material parameters estimated by nonlinear regression using these four methods. We also examined the dependency of the predicted parameters on the relative size of the pipette to the cell (described as R_p/R_c, the ratio of the pipette radius, R_p, to that of the cell, R_c) for all the tested cells, as this is a variable that has been shown to impact material parameter estimates (Haider and Guilak, 2002; Zhou et al., 2005).

The effect of loading rate was assessed using the standard half-space model, the superposition half-space model, and the inverse FE method to evaluate the experimental data of individual cells tested with 2 or 8 s loading periods. In the half-space model the pressure was applied instantaneously and in the superposition half-space and FE models the pressure was ramped over the actual loading period. Paired comparisons were made on the goodness of fit and the material parameter estimates.

2.6. Statistics

The goodness of fits were evaluated using the R-squared value (Draper and Smith, 1981). Paired and unpaired t-tests were used to determine statistical significance as appropriate. Linear regression was performed using SigmaStat (Systat Software Inc, San Jose, CA). Data are presented as the mean $\pm$ standard deviation.

3. Results

3.1. Inverse FE method validation

To confirm the robustness of the inverse FE method, nonlinear regression was performed on the experimental deformation history of one VIC. Four tests were performed with different ratios of the initial guesses to the 'target' material parameters (Table 1). Convergence of the cost function was achieved for all four cases (Fig. 1), and the difference of the optimized parameters was within 6% (Table 1).

3.2. Comparison of the analytical and numerical model predictions

Both the analytical standard half-space model and inverse FE models fit the experimental data well based on an assumption of instantaneous loading (Table 2), with a slightly better fit with the standard half-space model evident during the early creep phase (Fig. 2a). There were significant differences in G_0 and α_1 determined by the three analytical methods and the inverse FE method when compared on a paired, individual cell basis ($p < 0.001$; Table 2). However, when the average properties were compared on a whole population-basis by unpaired t-tests, G_0 predicted by the Zhou cell-size-corrected model was statistically indistinguishable from that predicted by the inverse FE method, and α_1 from the three analytical forms was not significantly different from that predicted by the inverse FE method. No significant differences were found in τ regardless if the comparison was made on an individual cell or population-basis.

To test the dependency of the parameter estimates on cell-size, the material parameters predicted by the inverse FE method were normalized to those predicted by the standard half-space model and plotted versus R_p/R_c for each cell. The inverse FE method stiffness values were greater than those predicted by the half-space model, and were linearly dependent on the R_p/R_c ratio with a good fitting quality ($R^2 \geq 0.74$) over the range of cell-sizes tested

Please cite this article as: Zhao, R., et al., Comparison of analytical and inverse finite element approaches to estimate cell viscoelastic properties by micropipette aspiration. Journal of Biomechanics (2009), doi:10.1016/j.jbiomech.2009.07.035

Table 1
Optimized material parameters determined by the inverse finite element method for different initial guesses.

	Initial value	Optimized value	Initial/Optimized	Iterations	SSR[a]
G_0 (Pa)	1066	536	2.0	12	1.6E-03
α_1	0.16	0.33	0.5		
$\tau\ (1-\alpha_1)$ (s)	1.4	2.6	0.5		
G_0 (Pa)	266	534	0.5	9	1.6E-03
α_1	0.64	0.32	2.0		
$\tau\ (1-\alpha_1)$ (s)	5.7	2.6	2.2		
G_0 (Pa)	1066	544	2.0	7	2.0E-03
α_1	0.64	0.34	1.9		
$\tau\ (1-\alpha_1)$ (s)	5.3	2.5	2.1		
G_0 (Pa)	266	530	0.5	16	1.6E-03
α_1	0.16	0.32	0.5		
$\tau\ (1-\alpha_1)$ (s)	1.4	2.6	0.5		

[a] Sum of squared residual errors.

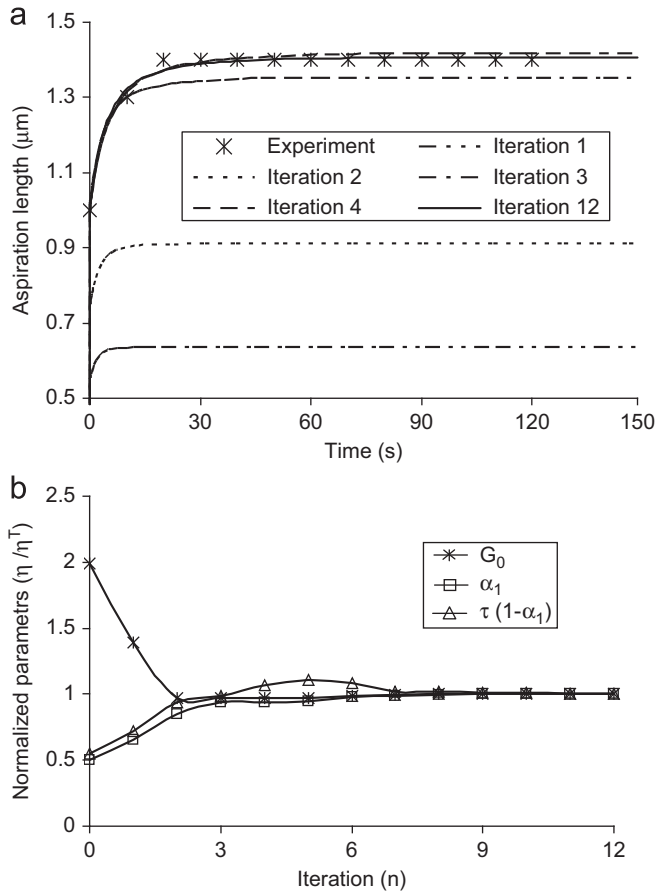

Fig. 1. Optimization process using the inverse FE method to analyze experimental data from one cell. The (a) initial, improved and optimized deformation history curves, and (b) convergence history are shown. Initial guesses correspond to those in the first three rows of Table 1.

(R_p/R_c=0.40–0.66). This linear dependency held for all the cells tested regardless of the loading rate (Fig. 3a). The slope of the linear regression line was different from zero ($p<0.001$), indicating that the dependency of normalized stiffness on R_p/R_c was statistically significant. The normalized values of other parameters (α_1, τ) were also significantly dependent on the R_p/R_c ratio ($p<0.001$), although the goodness of fit for these parameters was much poorer ($R^2 \leq 0.44$) (Fig. 3b and c).

3.3. Comparison of instantaneous versus finite loading rate

Experimental deformation curves obtained for ramp loading periods of 2 and 8 s were fit using the standard half-space model assuming instantaneous loading and the superposition half-space model with actual loading duration (Fig. 2b; Table 3). All of the estimated viscoelastic parameters were significantly different for instantaneous versus finite loading rates when compared on individual cell (paired) basis, for both 2 and 8 s loading periods ($p<0.05$; Table 3). However, when comparing the whole population of cells in each loading group by unpaired statistical tests, the differences in parameters between instantaneous versus ramped loading analytical models were not significant, except marginally for τ for the longer loading period (Table 3).

Comparison of the superposition half-space model and inverse FE models with actual loading periods showed significant differences in G_0 and α_1 for the short loading period when compared on an individual cell basis, but only G_0 tended towards being significantly different (p=0.064) when compared on population-basis by unpaired t-tests (Table 3). No significant differences were found in τ regardless if the comparison was made on an individual cell or population-basis. For cells tested with 8 s loading period, there were significant differences in G_0 and τ between the superposition half-space model and the inverse FE method regardless if the comparison was made on an individual cell or population-basis. A significant difference in α_1 was detected only on an individual cell basis (Table 3).

4. Discussion

Previous studies have demonstrated that analytical and numerical models of MA predict different material parameters (Aoki et al., 1997; Alexopoulos et al., 2003; Baaijens et al., 2005; Zhou et al., 2005; Boudou et al., 2006). However, these simulation-based studies did not account for the inherent experimental and biological variability of real experimental data. The approach used here, combining experimental data from a population of several cells and an inverse finite element method, allowed us to assess statistically if the differences between analytical and numerical material parameter estimates are significant and if experimental variability for typical test conditions masks these differences. We found that analytical and numerical estimates of material parameters based on paired analyses of individual cells generally do differ significantly, even when the analytical models were modified to account for finite cell-size. However, when population-averaged material parameters were compared, differences between the analytical and numerical estimates were

Please cite this article as: Zhao, R., et al., Comparison of analytical and inverse finite element approaches to estimate cell viscoelastic properties by micropipette aspiration. Journal of Biomechanics (2009), doi:10.1016/j.jbiomech.2009.07.035

Table 2
Comparisons of fitting quality and material parameters determined by analytical half-space models and inverse finite element method.

	Half-space model	Finite-thickness-corrected model (Boudou et al.)	Cell-size-corrected model (Zhou et al.)	Instantaneous inverse FE method
R^2	0.97 ± 0.03	N/A	N/A	0.95 ± 0.03
G_0 (Pa)	446 ± 123[b,e]	468 ± 131[b,e]	697 ± 264[c,f]	724 ± 271
α_1	0.45 ± 0.14[b,f]	0.45 ± 0.14[b,f]	0.45 ± 0.14[c,f]	0.52 ± 0.17
τ (s)	27.7 ± 20.5[d,f]	N/A	N/A	28.6 ± 30.9
G_∞ (Pa)[a]	232 ± 18	243 ± 20	353 ± 55	314 ± 80

[a] Long-term shear modulus $G_\infty = G_0 (1 - \alpha_1)$.
[b] $p < 0.01$ by paired t-test compared with inverse FE method prediction.
[c] $p < 0.06$ by paired t-test compared with inverse FE method prediction.
[d] $p > 0.84$ by paired t-test compared with half-space model prediction.
[e] $p < 0.06$ by unpaired t-test compared with inverse FE method prediction.
[f] $p > 0.39$ by unpaired t-test compared with inverse FE method prediction.

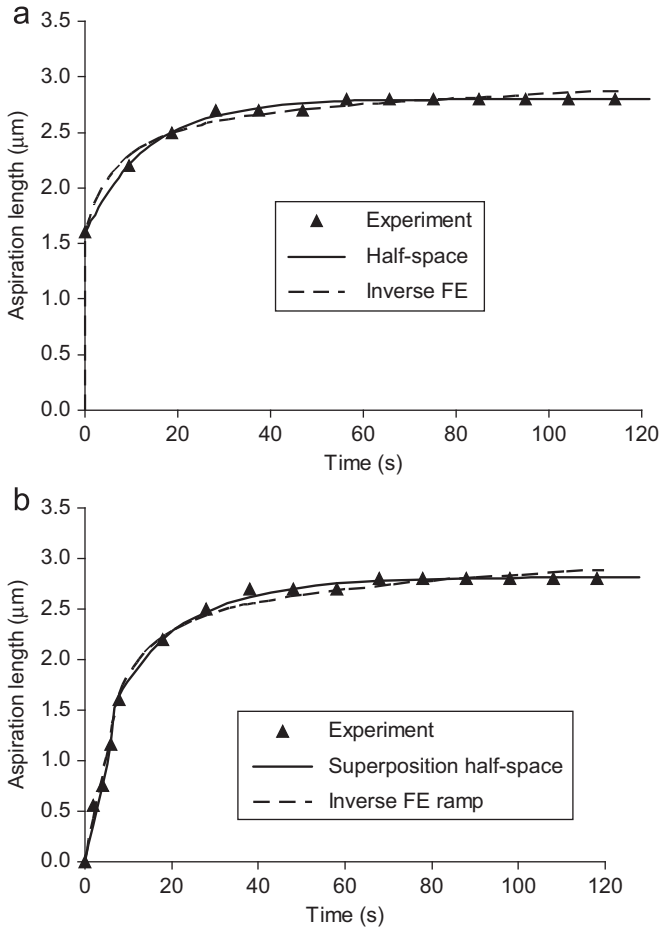

Fig. 2. The experimental deformation history of a typical VIC and the nonlinear regression curves determined by (a) standard half-space model and the inverse FE method assuming instantaneous loading; and (b) superposition half-space model and the inverse FE method under a linear ramp loading period of 8 s.

largely masked by cell-to-cell variability. In support of previous analytical results, we also found that viscoelastic parameters determined by MA for individual cells are significantly sensitive to finite versus instantaneous loading rate. However, for short loading periods, population-averaged estimates based on instantaneous versus finite loading periods and between analytical and numerical models were generally statistically indistinguishable.

The comparison of individual cell mechanical properties estimated analytically and numerically was enabled by the inverse FE method. A consistent finding was that the fitting quality of the load curve predicted with the inverse FE method was excellent, but often slightly lower than that of the half-space model. This was likely due to the geometrical and material constraints in the FE model that restrict the shape of the FE regression curve, particularly in the transition from the elastic to creep phase. Another difference between the half-space and FE models was that while both implemented viscoelastic material constitutive models, the FE method was based on finite strain, whereas the half-space model assumed infinitesimal strain. The large deformation of the cell, particularly around the fillets, suggests that the finite strain implementation is more appropriate (see Supplemental Material). While the current model was found to fit the experimental data very well, alternate material constitutive models, including those that account for cell compressibility (Baaijens et al., 2005) and inhomogeneity due to the nucleus (Guilak et al., 2000), are readily implemented in the inverse FE approach and may improve the fit accuracy.

The shear moduli estimated by the standard half-space model were significantly lower than those predicted by the inverse FE method, regardless if the comparison was made on an individual cell basis or as a whole population of cells. In the half-space model, the aspiration length of a cell is attributed solely to straining of the material, whereas the aspiration length in the FE model is contributed by both straining of the material and translation of the cell. Since the portion of aspiration length contributed by material straining is inversely proportional to the predicted shear modulus, the half-space model predicts a lower shear modulus (Supplemental Fig. S4). This phenomenon was first reported by Haider and Guilak (2002). Differences in α_1 predicted by the two methods were only statistically different when compared on a paired (individual cell) basis and not when the whole population was compared. Thus, while the standard half-space and inverse FE method predictions of α_1 are inherently different, cell-to-cell variability in the viscoelastic response masks these differences. Interestingly, differences in the estimates of τ were never significant, suggesting this parameter is insensitive to the estimation method.

Regression analyses demonstrated that the differences in the viscoelastic parameters predicted by the standard half-space model and the inverse FE method were significantly dependent on cell-size. The strongest relationships were those between cell-size and the differences in the instantaneous and equilibrium shear moduli. Correlations between cell-size and the predicted relaxation modulus and creep time constant were weaker ($R^2 < 0.46$) due to cell-to-cell variability, but were statistically significant. These relationships were independent of experimental loading rate and are expected to be independent of cell type. While the effect of cell-size can be minimized experimentally by reducing the pipette size, this can be technically challenging, both in terms of pipette manufacture and imaging requirements. Alternatively, analytical relationships derived from large-scale parametric FE analyses to account for finite sample

Please cite this article as: Zhao, R., et al., Comparison of analytical and inverse finite element approaches to estimate cell viscoelastic properties by micropipette aspiration. Journal of Biomechanics (2009), doi:10.1016/j.jbiomech.2009.07.035

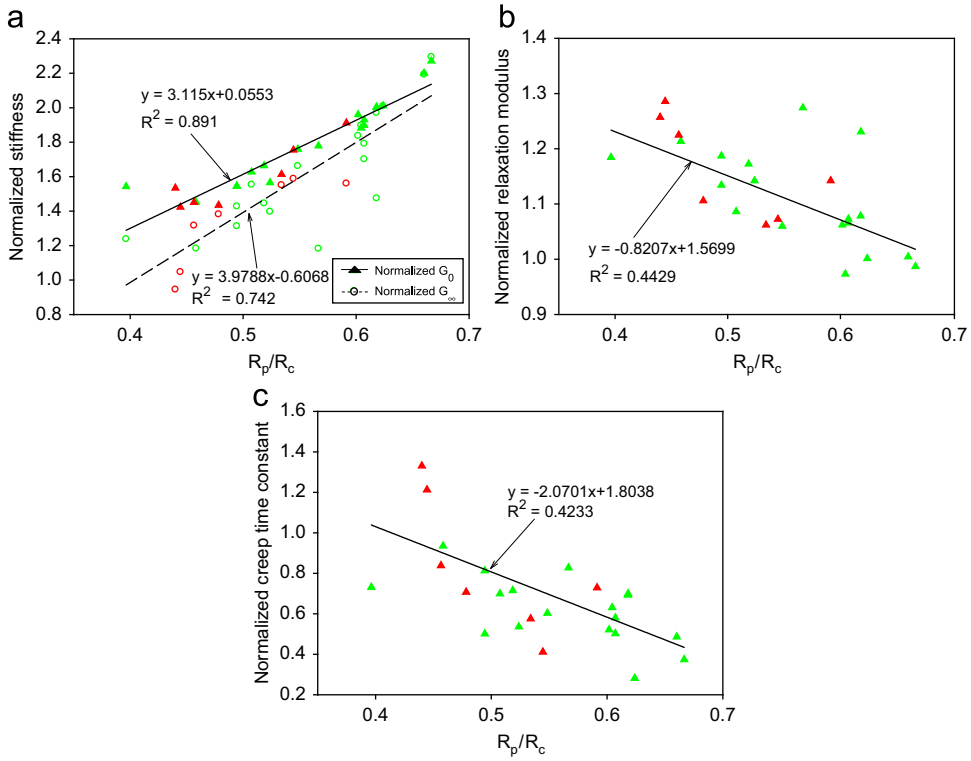

Fig. 3. The linear dependency of the (a) normalized instantaneous and long-term shear moduli; (b) normalized dimensionless relaxation modulus; and (c) normalized creep time constant on the ratio of the pipette to cell radius (R_p/R_c). Normalized parameters are defined as the ratio of the parameters estimated by the inverse FE method to that estimated by the standard half-space model. Red markers indicate 2 s loading period group; green, 8 s loading period. (For interpretation of the references to color in this figure legend, the reader is referred to the web version of this article.)

Table 3
Comparisons of the effect of loading rate on the fitting quality and material parameters determined by the half-space and inverse FE models.

	2 s loading period			8 s loading period		
	Half-space	Superposition half-space	Ramp inverse FE method	Half-space	Superposition half-space	Ramp inverse FE method
R^2	0.97 ± 0.03	0.99 ± 0.01	0.95 ± 0.03	0.97 ± 0.04	0.99 ± 0.01	0.98 ± 0.01
G_0 (Pa)	446 ± 123[a,d]	470 ± 142	804 ± 382[a,c]	444 ± 132[a,d]	505 ± 170	1087 ± 546[a,c]
α_1	0.45 ± 0.14[a,d]	0.47 ± 0.14	0.55 ± 0.18[a,d]	0.44 ± 0.11[a,d]	0.50 ± 0.13	0.58 ± 0.18[a,d]
τ (s)	27.7 ± 20.5[a,d]	29.1 ± 21.2	27.2 ± 30.4[b,d]	18.0 ± 6.9[a,c]	25.2 ± 10.7	11.3 ± 8.7[a,c]
G_∞ (Pa)	232 ± 18	232 ± 18	314 ± 80	246 ± 74	245 ± 74	407 ± 172

[a] $p < 0.05$ compared with superposition half-space model by paired t-test.
[b] $p > 0.63$ compared with superposition half-space model by paired t-test.
[c] $p < 0.064$ compared with superposition half-space model by unpaired t-test.
[d] $p > 0.16$ compared with superposition half-space model by unpaired t-test.

thickness (Boudou et al., 2006) and finite cell-size (Zhou et al., 2005) can be used. We found significant differences between each of these models and the inverse FE model predictions on an individual cell basis. However, the Zhou model predictions for both G_0 and α_1 were statistically indistinguishable from the inverse FE model estimates when the entire cell population was considered. Thus, the relationships proposed by Zhou et al., which account for the R_p/R_c ratio, closely approximate the inverse FE method if the instantaneous and equilibrium moduli of a population of cells are of interest.

The instantaneous moduli and time constants estimated in our study using the half-space model with instantaneous loading agree well with those reported by Merryman et al. (2009) for aortic valve interstitial cells. However, the equilibrium moduli measured in their study were lower than those determined in the current study. This discrepancy may be explained by the fact that they used pipettes significantly larger than those used here (7–9 μm inner diameter, resulting in an estimated R_p/R_c ratio > 0.5) and relatively large pipettes allow longer creep deformation to develop (Zhou et al., 2005). Another potential difference between the two studies is that we used freshly isolated VICs, whereas Merryman et al. measured the properties of subcultured cells. VICs undergo myofibroblast differentiation on rigid tissue culture polystyrene (Pho et al., 2008; Yip et al., 2009), which is accompanied by a change in their mechanical properties that persists even after detachment from the culture substrate (K. Wyss and C.A. Simmons, unpublished observations).

Practical issues require that the pressure in MA experiments be applied over a finite time. Merryman et al. (2009) accounted for finite MA loading rate by including Boltzmann superposition in the half-space standard linear solid model. In their experiments, a pressure of ~520 kPa was applied over an average ramp loading period of ~2.5 s. They observed differences in the properties predicted assuming instantaneous versus ramp loading, but did not assess if these differences were statistically significant.

Please cite this article as: Zhao, R., et al., Comparison of analytical and inverse finite element approaches to estimate cell viscoelastic properties by micropipette aspiration. Journal of Biomechanics (2009), doi:10.1016/j.jbiomech.2009.07.035

For loading periods of 2 or 8 s, we observed that all material parameters were significantly sensitive to the instantaneous versus finite loading assumption when compared on a single cell basis. For cell populations, the differences between instantaneous versus ramped loading were not significant for 2 s loading periods. Thus for short, but experimentally attainable loading periods of 2 s (corresponding here to a loading rate of $\sim$250 kPa/s), population variability masks differences that result from the assumption of instantaneous loading. Comparison of the material parameters estimated by the superposition half-space and inverse FE model showed similar trends: for short loading periods, individual cell differences between the models were generally masked on a population-basis. The exception was G_0 ($p < 0.064$), likely because the superposition half-space model did not correct for cell-size.

In conclusion, inherent differences in the half-space and finite element models yield different cell viscoelastic material parameters estimated from MA data. However, in situations in which short loading periods (≤ 2 s) and small pipette to cell radius ratios (< 0.4) can be achieved, experimental variability and heterogeneity in cell properties mask model-dependent differences, resulting in standard half-space model parameter estimates that are statistically indistinguishable from those predicted numerically. Extensions to the standard half-space model that account for finite cell-size (Zhou et al., 2005) or finite loading periods (Merryman et al., 2009) provide accurate population-based material parameter estimates over a wider range of experimental conditions, and therefore are recommended.

Conflict of interest statement

There are no conflicts of interest to report.

Acknowledgements

We acknowledge support from the Natural Sciences and Engineering Research Council of Canada, the Ontario Early Researcher Award (to CAS), and the Canada Research Chair in Mechanobiology (to CAS).

Appendix. Supporting Information

Supplementary data associated with this article can be found in the online version at doi:10.1016/j.jbiomech.2009.07.035.

References

ABAQUS, 2006. ABAQUS Analysis User's Manual (version 6.6). ABAQUS, Inc., Providence, RI, USA.

Alexopoulos, L.G., Haider, M.A., Vail, T.P., Guilak, F., 2003. Alterations in the mechanical properties of the human chondrocyte pericellular matrix with osteoarthritis. Journal of Biomechanical Engineering 125 (3), 323–333.

Aoki, T., Ohashi, T., Matsumoto, T., Sato, M., 1997. The pipette aspiration applied to the local stiffness measurement of soft tissues. Annals of Biomedical Engineering 25 (3), 581–587.

Baaijens, F.P.T., Trickey, W.R., Laursen, T.A., Guilak, F., 2005. Large deformation finite element analysis of micropipette aspiration to determine the mechanical properties of the chondrocyte. Annals of Biomedical Engineering 33 (4) 494–501.

Boudou, T., Ohayon, J., Arntz, Y., Finet, G., Picart, C., Tracqui, P., 2006. An extended modeling of the micropipette aspiration experiment for the characterization of the Young's modulus and Poisson's ratio of adherent thin biological samples: numerical and experimental studies. Journal of Biomechanics 39 (9) 1677–1685.

Darling, E.M., Topel, M., Zauscher, S., Vail, T.P., Guilak, F., 2008. Viscoelastic properties of human mesenchymally-derived stem cells and primary osteoblasts, chondrocytes, and adipocytes. Journal of Biomechanics 41, 454–464.

Draper, N.R., Smith, H., 1981. Applied Regression Analysis, second ed John Wiley and Sons, New York.

Guilak, F., Tedrow, J.R., Burgkart, R., 2000. Viscoelastic properties of the cell nucleus. Biochemical and Biophysical Research Communications 269 (3) 781–786.

Guilak, F., Ting-Beall, H.P., Baer, A.E., Trickey, W.R., Erickson, G.R., Setton, L.A., 1999. Viscoelastic properties of intervertebral disc cells—identification of two biomechanically distinct cell populations. Spine 24 (23), 2475–2483.

Haider, M.A., Guilak, F., 2002. An axisymmetric boundary integral model for assessing elastic cell properties in the micropipette aspiration contact problem. Journal of Biomechanical Engineering 124, 584–595.

Hochmuth, R.M., 2000. Micropipette aspiration of living cells. Journal of Biomechanics 33 (1), 15–22.

Kyriacou, S.K., Shah, A.D., Humphery, J.D., 1997. Inverse finite element characterization of nonlinear hyperelastic membranes. Journal of Applied Mechanics 64, 257–262.

Lei, F., Szeri, A.Z., 2007. Inverse analysis of constitutive models: biological soft tissues. Journal of Biomechanics 40, 936–940.

Merryman, W.D., Bieniek, P.D., Guilak, F., Sacks, M.S., 2009. Viscoelastic properties of the aortic valve interstitial cell. Journal of Biomechanical Engineering 131 (4), 041005.

Pho, M., Lee, W., Watt, D.R., Laschinger, C., Simmons, C.A., McCulloch, C.A., 2008. Cofilin is a marker of myofibroblast differentiation in cells from porcine aortic cardiac valves. American Journal of Physiology—Heart and Circulatory Physiolology 294 (4), H1767–H1778.

Rowat, A.C., Lammerding, J., Ipsen, J.H., 2006. Mechanical properties of the cell nucleus and the effect of emerin deficiency. Biophysical Journal 91, 4649–4664.

Sato, M., Theret, D.P., Wheeler, L.T., Ohshima, N., Nerem, R.M., 1990. Application of the micropipette technique to the measurement of cultured porcine aortic endothelial cell viscoelastic properties. Journal of Biomechanical Engineering 112 (3), 268.

Theret, D.P., Levesque, M.J., Sato, M., Nerem, R.M., Wheeler, L.T., 1988. The application of a homogeneous half-space model in the analysis of endothelial cell micropipette measurements. Journal of Biomechanical Engineering 110 (3), 190–199.

Trickey, W.R., Lee, G.M., Guilak, F., 2000. Viscoelastic properties of chondrocytes from normal and osteoarthritic human cartilage. Journal of Orthopaedic Research 18 (6), 891–898.

Vaziri, A., Mofrad, M.R.K., 2007. Mechanics and deformation of the nucleus in micropipette aspiration experiment. Journal of Biomechanics 40, 2053–2062.

Ward, K.A., Li, W.-I., Zimmer, S., Davis, T., 1991. Viscoelastic properties of transformed cells: role of tumor cell progression and metastasis formation. Biorheology 28, 301–313.

Yip, C.Y.Y., Chen, J.-H., Zhao, R., Simmons, C.A., 2009. Calcification by valve interstitial cells is regulated by the stiffness of the extracellular matrix. Arteriosclerosis, Thrombosis, and Vascular Biology 29, 936–942.

Zhou, E.H., Lim, C.T., Quek, S.T., 2005. Finite element simulation of the micropipette aspiration of a living cell undergoing large viscoelastic deformation. Mechanics of Advanced Materials and Structures 12 (6), 501–512.

Please cite this article as: Zhao, R., et al., Comparison of analytical and inverse finite element approaches to estimate cell viscoelastic properties by micropipette aspiration. Journal of Biomechanics (2009), doi:10.1016/j.jbiomech.2009.07.035